


# *In vitro* metabolic profiling of methylenedioxy-substituted synthetic cathinones for enhanced detection in urine sample analysis

Ya-Ling Yeh <sup>a,b</sup>, Chin-Lin Hsieh <sup>c</sup>, Yi-Jia Huang <sup>a</sup>, Yu-Hsiang Chang <sup>c</sup>,  
Sheng-Meng Wang <sup>a,\*</sup> 

<sup>a</sup> Department of Forensic Science, Central Police University, Taoyuan City, Taiwan, ROC

<sup>b</sup> Forensic Science Center, Taoyuan Police Department, Taoyuan City, Taiwan, ROC

<sup>c</sup> Forensic Science Center, Criminal Investigation Bureau, National Police Agency, Taipei City, Taiwan, ROC

## Abstract

Synthetic cathinones are a widely abused class of new psychoactive substances that pose significant challenges in forensic toxicology owing to their complex metabolic pathways and lack of verified reference standards. This study investigated the *in vitro* metabolism of nine methylenedioxy-substituted synthetic cathinones, including methylone and eight structural isomers, which were categorized into three groups: Group 1 (dimethylone, ethylone, and butylone), Group 2 (dibutylone, pentylone, and eutylone), and Group 3 (*N*-ethylpentylone and dipentylone). Pooled human liver microsomes, cytosol, and uridine diphosphate glucuronic acid were used to identify phase I and II metabolites by liquid chromatography–quadrupole time-of-flight mass spectrometry. Key pathways included *N*-dealkylation,  $\beta$ -ketone reduction, aliphatic hydroxylation, demethylenation, and glucuronide conjugation, with the analytes containing *N,N*-dimethylamino moieties showing higher *N*-dealkylation and  $\beta$ -ketone reduction ratios. Metabolic differences were semiquantitatively assessed using peak area ratios, which revealed relative trends among the analytes. Differences in the retention times and mass spectral fragmentation patterns enabled effective isomer differentiation, which was validated using a metabolite database. Analysis of 29 urine samples confirmed that the metabolites generated from  $\beta$ -ketone reduction (M2) and demethylenation followed by *O*-methylation (M3-5) were reliable detection targets. For instance, even when the parent drug concentrations were as low as 11 ng/mL (semiquantitative peak area ratio ~70.0%) for methylone (M-6) and 23 ng/mL (semiquantitative peak area ratio ~2.9%) for dibutylone (DB-8), multiple metabolites were detected. These metabolites extended the detection window beyond Taiwan's legal threshold of 50 ng/mL. Overall, this study provides a unified comparison of the products of synthetic cathinone metabolism, and highlights the importance of metabolites as key markers for enhanced identification accuracy in forensic toxicology.

**Keywords:** Cathinone, Isomer, LC-QTOF-MS, Metabolism

## 1. Introduction

Between 2009 and 2023, 1240 new psychoactive substances (NPS), approximately four times the number of substances under international control, were reported in the United Nations Office on Drugs and Crime Early Warning Advisory System [1]. Although the overall range of NPS in the global market has remained relatively stable since

2018, a total of 618 substances were recorded in 2021 [1]. Some NPS appear for a short period and then disappear, either because they do not have much demand or because they are replaced by other NPS. Owing to the fluidity of NPS usage, maintaining monitoring efforts to keep pace with these trends is challenging. Few NPS are widely abused in the global market; instead, most are limited to a few countries or specific locations.

Received 9 October 2024; accepted 13 March 2025.

Available online 13 June 2025

\* Corresponding author at: Department of Forensic Science, Central Police University, No.56, Shuren Rd., Guishan Dist., Taoyuan City 333322, Taiwan, ROC.

E-mail address: wang531088@mail.cpu.edu.tw (S.-M. Wang).

<https://doi.org/10.38212/2224-6614.3543>

2224-6614/© 2025 Taiwan Food and Drug Administration. This is an open access article under the CC-BY-NC-ND license (<http://creativecommons.org/licenses/by-nc-nd/4.0/>).

Additionally, estimating the frequency or severity of NPS abuse is difficult. For example, one country may report the abuse of two “less severe” NPS, whereas another may report the abuse of one “very severe” NPS [2]. Over the past decade, a notable shift in global drug trafficking from opiates to synthetic stimulants, particularly cathinones, has been observed in Central Asia, Transcaucasia, and Eastern Europe. The increased sales of synthetic cathinones was fueled by the Russian-language darknet market Hydra, which dominated dark-web drug sales prior to its shutdown in 2022. This transition is reflected in drug seizure data, which show NPS and amphetamine-type stimulant seizures tripling and opiate seizures declining between 2019 and 2022 [1].

In Taiwan, the Ministry of Health and Welfare reported that 194 NPS had been identified as of September 2024 [3]. The most widely reported NPS were synthetic cathinones, followed by synthetic cannabinoids and phenethylamines. The rampant distribution of synthetic cathinones is of particular concern, as these drugs comprise eight of the top 10 detected NPS. In addition to eutylone ([Eu], 1-(1,3-benzodioxol-5-yl)-2-(ethylamino)butan-1-one), other commonly detected methylenedioxy-substituted synthetic cathinones include methylone ([M], 1-(1,3-benzodioxol-5-yl)-2-(methylamino)-1-propan-1-one), *N*-ethylpentylone ([NEP], 1-(1,3-benzodioxol-5-yl)-2-(ethylamino)pentan-1-one), ethylone ([E], 1-(1,3-benzodioxol-5-yl)-2-(ethylamino)propan-1-one), dibutylone ([DB], 1-(1,3-benzodioxol-5-yl)-2-(dimethylamino)butan-1-one), and dipentylone ([DP], 1-(1,3-benzodioxol-5-yl)-2-(dimethylamino)pentan-1-one) [3]. Owing to the widespread addition of polydrugs in instant coffee packets in Taiwan, which has resulted in multiple cases of poisoning or death [4], testing for emerging drugs is urgently needed. Urine testing primarily focuses on the parent drug; however, the metabolic pathways and metabolites of these drugs are also important research topics.

Our literature review of methylenedioxy-substituted synthetic cathinone metabolism highlights several key findings from both urine and *in vitro* studies. The main pathways include *N*-dealkylation,  $\beta$ -ketone reduction, demethylenation followed by *O*-methylation, and aliphatic hydroxylation, though their prevalence varies among compounds and studies. Kamata et al. [5,6] identified *N*-dealkylation and *O*-methylation as primary pathways for [M] in urine, while Uralets et al. [7] reported that [M], [E], butylone ([B], 1-(1,3-benzodioxol-5-yl)-2-(methylamino)butan-1-one), and pentylone ([P], 1-(1,3-benzodioxol-5-yl)-2-(methylamino)pentan-1-one)

primarily undergo  $\beta$ -ketone reduction followed by *N*-dealkylation, with few parent compounds detected. Phase II conjugation reactions were significant, with Kamata et al. [5] reporting that over 80% of metabolites were conjugates, and Zaitsev et al. [8] observing increased concentrations of *O*-methylation metabolites after acid hydrolysis. *In vitro* studies confirmed demethylenation as a dominant pathway, but also revealed minor metabolites unique to specific compounds, such as those from *N*-hydroxylation and aliphatic hydroxylation (Pedersen et al. [9]; Meyer et al. [10]). Mueller et al. [11] highlighted the importance of *S*-adenosylmethionine (SAM) for detecting *O*-methylation metabolites, underscoring key experimental limitations. Consistent findings across multiple cathinones (i.e., [DB], [Eu], [NEP], and [DP]) in both urine and *in vitro* studies demonstrate the complementary nature of these approaches, and provide a robust foundation for understanding the metabolism of methylenedioxy-substituted synthetic cathinones [12–16].

The detection of methylenedioxy-substituted synthetic cathinones in forensic toxicology has been extensively studied; however, challenges in achieving systematic metabolite profiling and addressing isomer differentiation remain. Most prior research has focused on individual metabolic pathways, offering insights into phase I and II metabolism but lack standardized comparisons across multiple analytes to evaluate relative metabolic trends. This study addresses these challenges by investigating the *in vitro* metabolisms of nine synthetic cathinones (i.e., [M], dimethylone ([DM], 1-(1,3-benzodioxol-5-yl)-2-(dimethylamino)propan-1-one), [E], [Eu], [B], [DB], [P], [NEP], and [DP]) using pooled human liver microsomes (pHLM) and cytosol under identical conditions. To facilitate glucuronidation, uridine diphosphate glucuronic acid (UDPGA) and alamethicin, a channel-forming peptide antibiotic, are included in the incubation system [17–19]. This approach enables the systematic assessment of phase I and II metabolic pathways, the direct comparison of relative metabolic trends, and the consolidation of a metabolic database capable of distinguishing structural isomers, which is a critical step for improving substance identification. Integration of the analysis of urine samples, in which substances such as [M], [DB], [NEP], and [DP] were identified, with the *in vitro* data further validated the detection targets, providing a comprehensive framework for synthetic cathinone analysis in forensic toxicology. Given the limitations of the current drug testing regulations in Taiwan, which focus on parent compounds and have a narrow detection window for synthetic cathinones,

this study highlights the utility of *in vitro* metabolism experiments for metabolite profiling. The data obtained will be expected to extend the detection window, while also enhancing the applicability of synthetic cathinone analysis in forensic toxicology. Furthermore, proposed approach aims to provide a comprehensive analytical model for similar synthetic cathinones, and to serve as a valuable reference for future identification efforts.

## 2. Materials and methods

### 2.1. Materials

Standards (1 mg/mL) of [M], [DM], [E], [B], [DB], [P], [Eu], [EP], and [DP] and internal standards (100 µg/mL) of mephedrone-*d*<sub>3</sub> and methylenedioxypyrovalerone (MDPV)-*d*<sub>8</sub> were obtained from Cerilliant Corporation (TX, USA). High-performance liquid chromatography-grade ethyl acetate, acetonitrile, and methanol were sourced from Honeywell Burdick & Jackson (MI, USA). Analytical-grade formic acid was purchased from Fisher Scientific (PA, USA). Sodium carbonate, sodium bicarbonate, and sodium hydroxide were supplied by Katayama Chemical Industries Corporation (OSA, Japan). Sodium dihydrogen phosphate was obtained from PanReac AppliChem (DA, Germany), while sodium hydrogen phosphate was obtained from J.T. Baker (NJ, USA). *S*-(5'-Adenosyl)-*L*-methionine chloride dihydrochloride (SAM) was sourced from Sigma–Aldrich (MA, USA). In addition, a 150-donor mixed-gender HLM pool (pHLM), a 150-donor mixed-gender human liver cytosol pool, nicotinamide adenine dinucleotide phosphate regenerating system solution A (NADPH A), NADPH regenerating system solution B (NADPH B), uridine 5'-diphospho-glucuronosyltransferase reaction mix solution A (UGT A), and UGT reaction mix solution B (UGT B) were obtained from Corning (NY, USA). Finally, 29 urine samples collected from individuals suspected of drug use were obtained from the Taoyuan Police Department in Taiwan in accordance with Taiwanese legal regulations, with all personal identifiers removed.

### 2.2. Instrumentation

Analytical methods similar to those used in our previous research were employed [16]. All analyses were performed using liquid chromatography–quadrupole time-of-flight mass spectrometry (LC-QTOF-MS). The LC system (1260, Agilent) was connected to an accurate quadrupole time-of-flight mass spectrometer (6530 B, Agilent). A packed LC

column (Poroshell 120 EC-C18, 3.0 × 100 mm, 2.7 µm, Agilent) was used, and the column temperature was maintained at 30 °C. The mobile phases consisted of 0.1% formic acid in water (A) and 0.1% formic acid in methanol (B). Gradient elution was performed, starting from 10% to 100% B over a duration of 10 min, with a total run time of 18 min, a flow rate of 0.4 mL/min, and an injection volume of 5 µL. Dual-source electrospray ionization MS was conducted in positive-ion mode with nitrogen as both the drying and nebulizer gas, maintaining specific voltage settings identical to those used in our previous study [16]. Mass calibration and all related settings followed the same established protocol.

### 2.3. *In vitro* phase I metabolism experiments

The incubation procedure of the *in vitro* phase I metabolism experiment was conducted according to Presley et al. [20,21] and our previous study [16] with some modifications. Each standard (1 mg/mL) was dried and reconstituted with deionized water to obtain a drug standard. Reaction solutions were then prepared from a drug standard (1 µL) with 100 mM phosphate buffer (Na<sub>2</sub>HPO<sub>4</sub>/NaH<sub>2</sub>PO<sub>4</sub>, 100 mM, pH 7.4, 81 µL), NADPH A (5 µL), NADPH B (1 µL), and pHLM (5 µL). Each reaction solution was thoroughly mixed and incubated at 37 °C in a shaking incubator for 1 h. Subsequently, the reaction solution was removed from the incubator and combined with 1 mM SAM (2 µL) and cytosol (5 µL). The obtained mixture, with a total volume of 100 µL, was thoroughly mixed and incubated at 37 °C in a shaking incubator for 2 h. Next, ice-cold acetonitrile (100 µL) was added to quench the reaction. The sample was then subjected to centrifuged at 21,379 RCF and 4.0 °C for 5 min. Finally, an aliquot (150 µL) of the supernatant was transferred to an autosampler vial for LC-QTOF-MS analysis.

### 2.4. *In vitro* phase I and II metabolism experiments

For the *in vitro* phase I and phase II metabolism experiments, the procedures described in Section 2.3 were performed to incubate the reaction solution with pHLM for 1 h and with cytosol for 1 h. The reaction solution was then removed from the incubator. Separately, pHLM (5 µL), deionized water (33 µL), and UGT B (40 µL) were mixed thoroughly and cooled in an ice bath for 15 min. This mixture was then warmed to ~25 °C and added to the reaction solution. Thereafter, NADPH A (5 µL), NADPH B (1 µL), and UGT A (16 µL) were added to

the reaction solution. The obtained mixture, with a total volume of 200  $\mu\text{L}$ , was thoroughly mixed and incubated at 37  $^{\circ}\text{C}$  in a shaking incubator for 2 h. Subsequently, ice-cold acetonitrile (100  $\mu\text{L}$ ) was added to quench the reaction. After centrifugation at 21,379 RCF and 4.0  $^{\circ}\text{C}$  for 5 min, an aliquot (150  $\mu\text{L}$ ) of the supernatant was transferred to an autosampler vial for LC-QTOF-MS analysis.

### 2.5. Pretreatment of the urine samples

Standard solutions of [M], [DB], and [NEP] were further diluted to concentrations of 10, 1, and 0.1  $\mu\text{g}/\text{mL}$  and used as the working standards. The mephedrone- $d_3$  and MDPV- $d_8$  solutions were also diluted to a concentration of 10  $\mu\text{g}/\text{mL}$  and used as working standards. The pretreatment of urine samples *via* liquid–liquid extraction was validated before analysis. The dynamic ranges of [M], [DB], and [NEP] were 5–1000, 2.5–1000, and 50–1000 ng/mL, respectively. During the experiment, an aliquot (500  $\mu\text{L}$ ) of a buffer solution ( $\text{Na}_2\text{CO}_3/\text{NaHCO}_3$ , 0.5 M, pH 9) was added to each urine sample (500  $\mu\text{L}$ ) containing 50 ng/mL mephedrone- $d_3$  and MDPV- $d_8$  as internal standards. The resulting solutions were extracted twice with ethyl acetate (5 mL) and then subjected to centrifugation at 4414 RCF for 5 min. After this time, the supernatant was transferred to a

clean tube and evaporated to near-dryness in a 40  $^{\circ}\text{C}$  bath under a gentle stream of nitrogen gas. Finally, the samples were reconstituted in mobile phase A (200  $\mu\text{L}$ ) for LC-QTOF-MS analysis. One [DP] urine sample was also subjected to the same pretreatment method. However, only the relative metabolite content in this sample was evaluated because method validation was not performed to establish the dynamic range for this analyte; thus, quantitative analysis could not be conducted.

### 2.6. Identification of the *in vitro* and *in vivo* samples

Potential metabolites were identified based on the literature [12–15] and on our previous research [16]. Phase I metabolites were classified according to the following pathways: (1) *N*-dealkylation, (2)  $\beta$ -ketone reduction, (3) demethylenation, (4) aliphatic hydroxylation, and (5) *O*-methylation. Phase II pathways, including glucuronic acid conjugation, were labeled as “g.” The possible phase I and phase II metabolic pathways of the nine analytes and their metabolites are shown in Fig. 1. The compound names, formulae, and accurate masses of potential metabolites were established in the Personal Compound Databases and Library (PCDL) for further analysis using Agilent MassHunter Qualitative

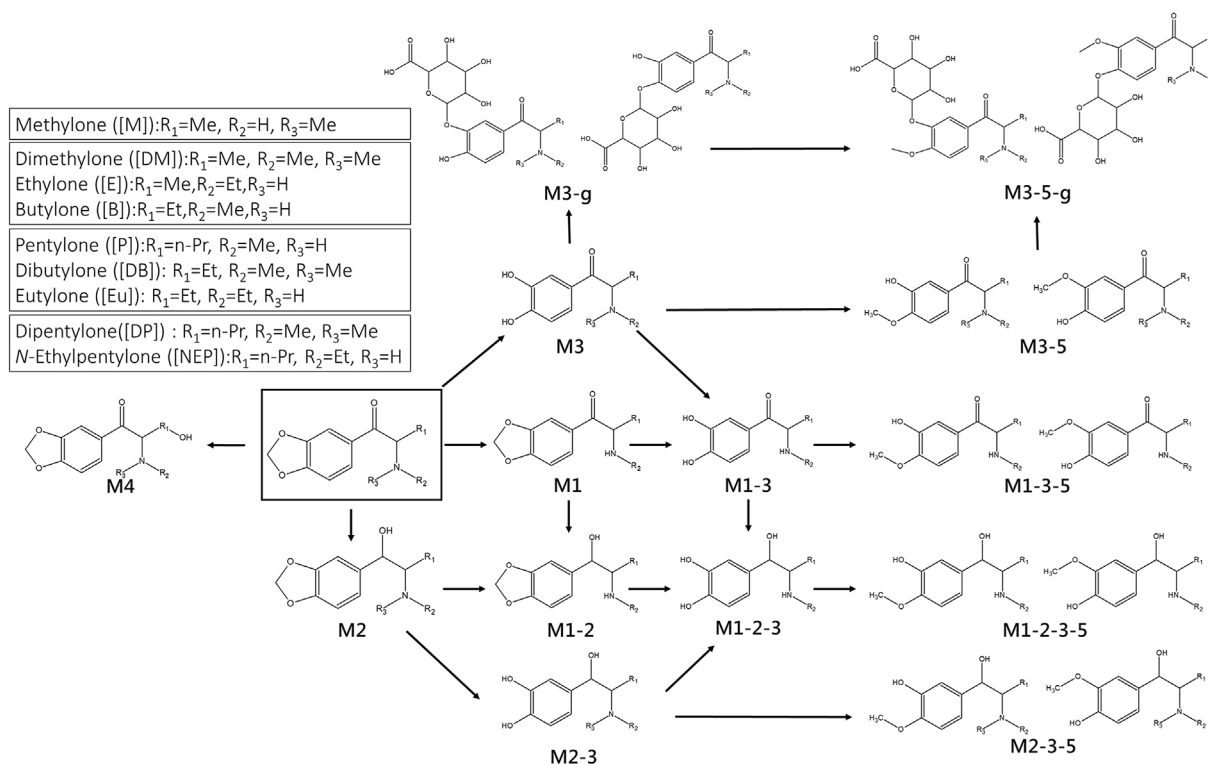


Fig. 1. Phase I and II metabolic pathways for the nine analytes and their metabolites investigated in this study. The metabolic pathways include *N*-dealkylation (1),  $\beta$ -ketone reduction (2), demethylenation (3), aliphatic hydroxylation (4), *O*-methylation (5), and glucuronide conjugation (g).



Analysis software (version B.07.00) and MassHunter MassProfiler (B.07.02).

As in our previous study [16], the “MS feature extraction (MFE)” algorithm in MassProfiler was used to group isotopes of the same neutral molecule into one composite feature, which was then compared with the PCDL to identify potential metabolites. The “Find Compounds by Formula” function in Qualitative Analysis (mass match score,  $\geq 60$ ; tolerance,  $\pm 15$  ppm) was used to manually review potential metabolites based on the extracted ion chromatograms. Additionally, MS/MS spectra for collision energies (CEs) of 10, 20, and 40 eV were extracted with a precursor tolerance of  $\pm 20$  ppm. After the metabolite results from the *in vitro* metabolism experiment were verified, the corresponding MS/MS spectra were incorporated into the PCDL.

### 2.7. Semiquantitative peak area ratio calculations

Owing to the lack of reference standards for the absolute quantification of potential metabolites, we employed a relative ratio calculation method inspired by the semiquantitative ion current count approach described by Paul et al. [22], but used the peak area to compare the extent of metabolism and assess the relative analyte abundance. The peak area ratio for each analyte was calculated as the percentage of its peak area relative to the total peak area, where the total peak area was defined as the sum of the peak areas of the parent compound and all detected metabolites. This method allowed us to evaluate the relative contributions of each compound and its metabolites under the given experimental conditions.

The calculated ratios were visualized in a heatmap, with the color intensity representing the relative abundance of each metabolite, to enable comparison of the metabolic profiles of the analytes in both *in vitro* and *in vivo* samples. For the *in vitro* experiments, hierarchical clustering was performed using Ward's method with Euclidean distances, grouping analytes and metabolites based on their calculated ratios. This approach facilitated the identification of similarities and differences in the metabolic profiles of the studied compounds.

## 3. Results

### 3.1. *In vitro* phase I metabolites

In the *in vitro* phase I metabolism experiments, metabolites resulting from *N*-dealkylation (M1),  $\beta$ -ketone reduction (M2), demethylenation (M3), aliphatic hydroxylation (M4), and both

demethylenation and *O*-methylation (M3-5) were observed for all analytes. For [NEP], additional metabolites from *N*-dealkylation and  $\beta$ -ketone reduction (M1-2), as well as *N*-dealkylation, demethylenation, and *O*-methylation (M1-3-5), were detected. M3-5 emerged as the dominant metabolite across most analytes, indicating its significance in the metabolic profiling of methylenedioxy-substituted cathinones. These findings align with those of prior research, which identified *N*-dealkylation and demethylenation followed by *O*-methylation as the major metabolic pathways for this class of compounds [5,6,9–11].

Table 1 summarizes the results of the *in vitro* metabolism experiments for all analytes and their metabolites, including their formulae, retention times (RTs), monoisotopic masses, measures of  $[M + H]^+$ , mass errors (in ppm), and the main product ions observed at a CE of 20 eV. The mass error ranged from  $-7.58$  to  $7.54$  ppm for all compounds. Notably, metabolites from the  $\beta$ -keto reduction (M2) of [M], [DM], [E], [DB], [Eu], and [P] exhibited two peaks, likely owing to diastereomer formation, as supported by Zaitseva *et al* [23]. However, this diastereomeric phenomenon was not observed for [DP]M2 and [NEP]M2. Furthermore, two peaks with identical MS/MS spectra were observed for [E]M3.

The calculated peak area ratios of the nine analytes and their metabolites (diastereomeric compounds were combined) for phase I metabolism were obtained and summarized in a heatmap and hierarchical clustering dendrogram, as shown in Fig. 2. The calculated peak area ratios were 92.6% for [M], 91.6% for [E], 86.5% for [B], 85.2% for [Eu], 79.9% for [P], 79.8% for [NEP], 64.8% for [DM], 51.1% for [DB], and 29.4% for [DP]. These results indicate that the calculated peak area ratios of the analytes decrease with an increasing molecular weight. It was also found that analytes containing *N,N*-dimethylamino moieties (i.e., [DM], [DB], and [DP]) exhibited significantly lower proportions of their parent compounds, suggesting a higher propensity for *N*-dealkylation. This trend is consistent with literature findings that tertiary *N,N*-dialkylamino groups undergo sequential *N*-dealkylation [24], suggesting that analytes bearing *N,N*-dimethylamino moieties undergo more extensive dealkylation, leading to lower proportions of their corresponding parent compounds. [DP] displayed a distinct metabolic profile with a high M1 ratio of 27.2%. This finding highlights the critical role of *N*-dealkylation as the dominant pathway in such compounds, a trend that has not been explicitly quantified in prior studies. [DM] and [DB] showed

Table 1. In vitro phase I and II metabolism data for the nine analytes and their metabolites investigated in this study.

Parent analyte and metabolites		Formula	RT <sup>a</sup> (min)	Monoisotopic mass	Measure of [M+H] <sup>+</sup>	Mass error (ppm)	Main observed product ions (20 eV CE)	Detected <sup>b</sup>	
Methylone	Parent, [M]	C <sub>11</sub> H <sub>13</sub> NO <sub>3</sub>	5.28	208.0968	208.0970	0.96	190, 160, 132, 58	A	B
	[M]M1	C <sub>10</sub> H <sub>11</sub> NO <sub>3</sub>	5.03	194.0812	194.0817	2.58	176, 146, 118, 109, 91	A	B
	[M]M2	C <sub>11</sub> H <sub>15</sub> NO <sub>3</sub>	4.96/5.28	210.1125	210.1132	3.33	Not obtained	A	B
	[M]M3	C <sub>10</sub> H <sub>13</sub> NO <sub>3</sub>	2.01	196.0968	196.0971	1.53	178, 163, 160, 137, 132, 117, 58	A	
	[M]M4	C <sub>11</sub> H <sub>13</sub> NO <sub>4</sub>	6.62	224.0917	224.0925	3.57	149, 121, 74, 56	A	B
	[M]M3-5	C <sub>11</sub> H <sub>15</sub> NO <sub>3</sub>	4.03	210.1125	210.1129	1.90	192, 160, 132, 58	A	B
	[M]M3-5-g	C <sub>17</sub> H <sub>23</sub> NO <sub>9</sub>	1.54/2.23	386.1446	386.1437	−2.33	210, 192, 160, 137, 122, 58		B
	Parent, [DM]	C <sub>12</sub> H <sub>15</sub> NO <sub>3</sub>	5.35	222.1125	222.1126	0.45	177, 147, 149, 119, 91, 72	A	B
Dimethylone	[DM]M1, [M]	C <sub>11</sub> H <sub>13</sub> NO <sub>3</sub>	5.22	208.0968	208.0970	0.96	190, 160, 132, 58	A	B
	[DM]M2	C <sub>12</sub> H <sub>17</sub> NO <sub>3</sub>	4.99/5.35	224.1281	224.1282	0.45	206, 191, 135, 103, 72	A	B
	[DM]M3	C <sub>11</sub> H <sub>15</sub> NO <sub>3</sub>	3.95	210.1125	210.1125	0.00	147, 137, 119, 72	A	
	[DM]M4	C <sub>12</sub> H <sub>15</sub> NO <sub>4</sub>	6.23	238.1074	238.1074	0.00	178, 149, 72, 60	A	B
	[DM]M3-5	C <sub>12</sub> H <sub>17</sub> NO <sub>3</sub>	4.37	224.1281	224.1281	0.00	179, 151, 147, 119, 91, 72	A	B
	[DM]M3-5-g	C <sub>17</sub> H <sub>23</sub> NO <sub>9</sub>	1.98	386.1446	386.1438	−2.07	210, 72		B
	[DM]M3-5-g	C <sub>18</sub> H <sub>25</sub> NO <sub>9</sub>	1.67/2.48	400.1602	400.1602	0.00	224, 179, 147, 72		B
	Parent, [E]	C <sub>12</sub> H <sub>15</sub> NO <sub>3</sub>	5.74	222.1125	222.1129	1.80	204, 189, 174, 146, 72	A	B
Ethylone	[E]M1, [M]M1	C <sub>10</sub> H <sub>11</sub> NO <sub>3</sub>	5.01	194.0812	194.0815	1.55	176, 146, 118, 109, 91	A	B
	[E]M2	C <sub>12</sub> H <sub>17</sub> NO <sub>3</sub>	5.63/5.74	224.1281	224.1277	−1.78	206, 191, 177, 131, 103, 70	A	B
	[E]M3	C <sub>11</sub> H <sub>15</sub> NO <sub>3</sub>	1.38/2.73	210.1125	210.1126	0.48	192, 174, 163, 142, 72	A	
	[E]M4	C <sub>12</sub> H <sub>15</sub> NO <sub>4</sub>	7.13	238.1074	238.1075	0.42	149, 121, 117, 59	A	
	[E]M3-5	C <sub>12</sub> H <sub>17</sub> NO <sub>3</sub>	4.83	224.1281	224.1281	0.00	210, 206, 191, 175, 174, 146, 72	A	B
	[E]M3-5-g	C <sub>18</sub> H <sub>25</sub> NO <sub>9</sub>	1.85/2.97	400.1602	400.1617	3.75	224, 206, 174, 72		B
	Parent, [B]	C <sub>12</sub> H <sub>15</sub> NO <sub>3</sub>	6.30	222.1125	222.1127	0.90	204, 175, 174, 161, 146, 72	A	B
	[B]M1	C <sub>11</sub> H <sub>13</sub> NO <sub>3</sub>	6.18	208.0968	208.0970	0.96	190, 161, 160, 149, 132, 58	A	B
Butylone	[B]M2	C <sub>12</sub> H <sub>17</sub> NO <sub>3</sub>	5.99/6.18/6.30	224.1281	224.1274	−3.12	206, 177, 145, 135, 70	A	B
	[B]M3	C <sub>11</sub> H <sub>15</sub> NO <sub>3</sub>	3.72	210.1125	210.1126	0.48	192, 174, 163, 146, 123, 72	A	
	[B]M4	C <sub>12</sub> H <sub>15</sub> NO <sub>4</sub>	7.69	238.1074	238.1075	0.42	149, 121, 70	A	B
	[B]M3-5	C <sub>12</sub> H <sub>17</sub> NO <sub>3</sub>	5.38	224.1281	224.1279	−0.89	206, 191, 174, 146, 72	A	B
	[B]M3-5-g	C <sub>18</sub> H <sub>25</sub> NO <sub>9</sub>	2.36/3.92	400.1602	400.1601	−0.25	224, 206, 174, 72		B
	Parent, [DB]	C <sub>13</sub> H <sub>17</sub> NO <sub>3</sub>	6.37	236.1281	236.1284	1.27	191, 161, 149, 86	A	B
	[DB]M1, [B]	C <sub>12</sub> H <sub>15</sub> NO <sub>3</sub>	6.31	222.1125	222.1128	1.35	204, 175, 174, 161, 146, 72	A	B
	[DB]M2	C <sub>13</sub> H <sub>19</sub> NO <sub>3</sub>	6.06/6.34	238.1438	238.1442	1.68	220, 191, 145, 135, 86	A	B
Dibutylone	[DB]M3	C <sub>12</sub> H <sub>17</sub> NO <sub>3</sub>	4.15	224.1281	224.1282	0.45	179, 161, 151, 137, 123, 86	A	B
	[DB]M4	C <sub>13</sub> H <sub>17</sub> NO <sub>4</sub>	7.27	252.1230	252.1232	0.79	192, 177, 149, 121, 86	A	B
	[DB]M3-5	C <sub>13</sub> H <sub>19</sub> NO <sub>3</sub>	5.5	238.1438	238.1440	0.84	193, 161, 151, 86	A	B
	[DB]M3-5-g	C <sub>18</sub> H <sub>25</sub> NO <sub>9</sub>	3.49	400.1602	400.1601	−0.25	224, 179, 86		B
	[DB]M3-5-g	C <sub>19</sub> H <sub>27</sub> NO <sub>9</sub>	2.69/3.00/4.27	414.1759	414.1757	−0.48	238, 193, 161, 86		B
	Parent, [Eu]	C <sub>13</sub> H <sub>17</sub> NO <sub>3</sub>	6.6	236.1281	236.1285	1.69	218, 191, 188, 161, 149, 86	A	B
	[Eu]M1	C <sub>11</sub> H <sub>13</sub> NO <sub>3</sub>	6.18	208.0968	208.0969	0.48	190, 160, 149, 132, 117, 58	A	B
	[Eu]M2	C <sub>13</sub> H <sub>19</sub> NO <sub>3</sub>	6.41/6.60	238.1438	238.1439	0.42	220, 191, 145, 135, 86	A	B
Eutylone	[Eu]M3	C <sub>12</sub> H <sub>17</sub> NO <sub>3</sub>	4.37	224.1281	224.1283	0.89	206, 188, 177, 137, 123, 86	A	
	[Eu]M4	C <sub>13</sub> H <sub>17</sub> NO <sub>4</sub>	8.14	252.1230	252.1235	1.98	149, 121, 102, 56	A	B
	[Eu]M3-5	C <sub>13</sub> H <sub>19</sub> NO <sub>3</sub>	5.68	238.1438	238.1439	0.42	220, 191, 188, 176, 161, 151, 86	A	B
	[Eu]M3-5-g	C <sub>19</sub> H <sub>27</sub> NO <sub>9</sub>	2.86/4.48	414.1759	414.1759	0.00	238, 220, 188, 161, 86		B

(continued on next page)

Table 1. (continued)

Parent analyte and metabolites		Formula	RT <sup>a</sup> (min)	Monoisotopic mass	Measure of [M+H] <sup>+</sup>	Mass error (ppm)	Main observed product ions (20 eV CE)	Detected <sup>b</sup>	
Pentylone	Parent, [P]	C <sub>13</sub> H <sub>17</sub> NO <sub>3</sub>	7.32	236.1281	236.1285	1.69	218, 188, 175, 160, 149, 135, 86	A	B
	[P]M1	C <sub>12</sub> H <sub>15</sub> NO <sub>3</sub>	7.28	222.1125	222.1120	−2.25	204, 174, 149, 146, 135, 117, 72	A	B
	[P]M2	C <sub>13</sub> H <sub>19</sub> NO <sub>3</sub>	7.13/7.32	238.1438	238.1440	0.84	220, 177, 159, 135, 86	A	B
	[P]M3	C <sub>12</sub> H <sub>17</sub> NO <sub>3</sub>	5.44	224.1281	224.1283	0.89	206, 193, 188, 163, 137, 123, 86	A	
	[P]M4	C <sub>13</sub> H <sub>17</sub> NO <sub>4</sub>	8.88	252.1230	252.1239	3.57	149, 121, 102, 84	A	B
	[P]M3-5	C <sub>13</sub> H <sub>19</sub> NO <sub>3</sub>	6.44	238.1438	238.1438	0.00	220, 188, 177, 151, 86	A	B
	[P]M3-5-g	C <sub>19</sub> H <sub>27</sub> NO <sub>9</sub>	4.30/4.57/5.21	414.1759	414.1755	−0.97	238, 220, 188, 86		B
Dipentylone	Parent, [DP]	C <sub>14</sub> H <sub>19</sub> NO <sub>3</sub>	7.37	250.1438	250.1440	0.80	205, 175, 149, 135, 100	A	B
	[DP]M1, [P]	C <sub>13</sub> H <sub>17</sub> NO <sub>3</sub>	7.31	236.1281	236.1284	1.27	218, 188, 175, 160, 149, 135, 86	A	B
	[DP]M2	C <sub>14</sub> H <sub>21</sub> NO <sub>3</sub>	7.02	252.1594	252.1598	1.59	234, 191, 159, 135	A	B
	[DP]M3	C <sub>13</sub> H <sub>19</sub> NO <sub>3</sub>	5.60	238.1438	238.1432	−2.51	193, 175, 137, 123, 100	A	
	[DP]M4	C <sub>14</sub> H <sub>19</sub> NO <sub>4</sub>	8.10	266.1387	266.1393	2.25	206, 177, 149, 135, 121, 100, 60	A	B
	[DP]M3-5	C <sub>14</sub> H <sub>21</sub> NO <sub>3</sub>	6.53	252.1594	252.1597	1.19	207, 175, 151, 137, 100	A	B
	[DP]M3-g	C <sub>19</sub> H <sub>27</sub> NO <sub>9</sub>	5.17	414.1759	414.1754	−1.21	238, 220, 193, 137, 100		B
N-Ethylpentylone	[DP]M3-5-g	C <sub>20</sub> H <sub>29</sub> NO <sub>9</sub>	4.97/5.36	428.1915	428.1910	−1.17	252, 207, 175, 137, 100		B
	Parent, [NEP]	C <sub>14</sub> H <sub>19</sub> NO <sub>3</sub>	7.52	250.1438	250.1443	2.00	232, 202, 189, 175, 149, 135, 100	A	B
	[NEP]M1	C <sub>12</sub> H <sub>15</sub> NO <sub>3</sub>	7.26	222.1125	222.1126	0.45	204, 174, 149, 146, 135, 117, 72	A	B
	[NEP]M2	C <sub>14</sub> H <sub>21</sub> NO <sub>3</sub>	7.46	252.1594	252.1596	0.79	234, 191, 135, 70	A	B
	[NEP]M3	C <sub>13</sub> H <sub>19</sub> NO <sub>3</sub>	5.67	238.1438	238.1440	0.84	220, 202, 191, 177, 162, 137, 123, 100	A	
	[NEP]M4	C <sub>14</sub> H <sub>19</sub> NO <sub>4</sub>	9.29	266.1387	266.1387	0.00	149, 121, 98, 70	A	B
	[NEP]M1-3-5	C <sub>12</sub> H <sub>17</sub> NO <sub>3</sub>	6.36	224.1281	224.1281	0.00	206, 191, 174, 151, 137, 117, 72	A	B
	[NEP]M1-2	C <sub>12</sub> H <sub>17</sub> NO <sub>3</sub>	6.92	224.1281	224.1278	−1.34	206, 176, 150, 135	A	B
	[NEP]M3-5	C <sub>14</sub> H <sub>21</sub> NO <sub>3</sub>	6.62	252.1594	252.1598	1.59	234, 202, 191, 137, 100	A	B
	[NEP]M3-g	C <sub>19</sub> H <sub>27</sub> NO <sub>9</sub>	5.22	414.1759	414.1757	−0.48	238, 220, 202, 137, 100		B
	[NEP]M3-5-g	C <sub>20</sub> H <sub>29</sub> NO <sub>9</sub>	4.63/4.77/5.44	428.1915	428.1912	−0.7	252, 234, 202, 191, 137, 100		B

<sup>a</sup> RT: retention time.<sup>b</sup> A: Results for *in vitro* phase I metabolism. B: Results for *in vitro* phase I and II metabolism.

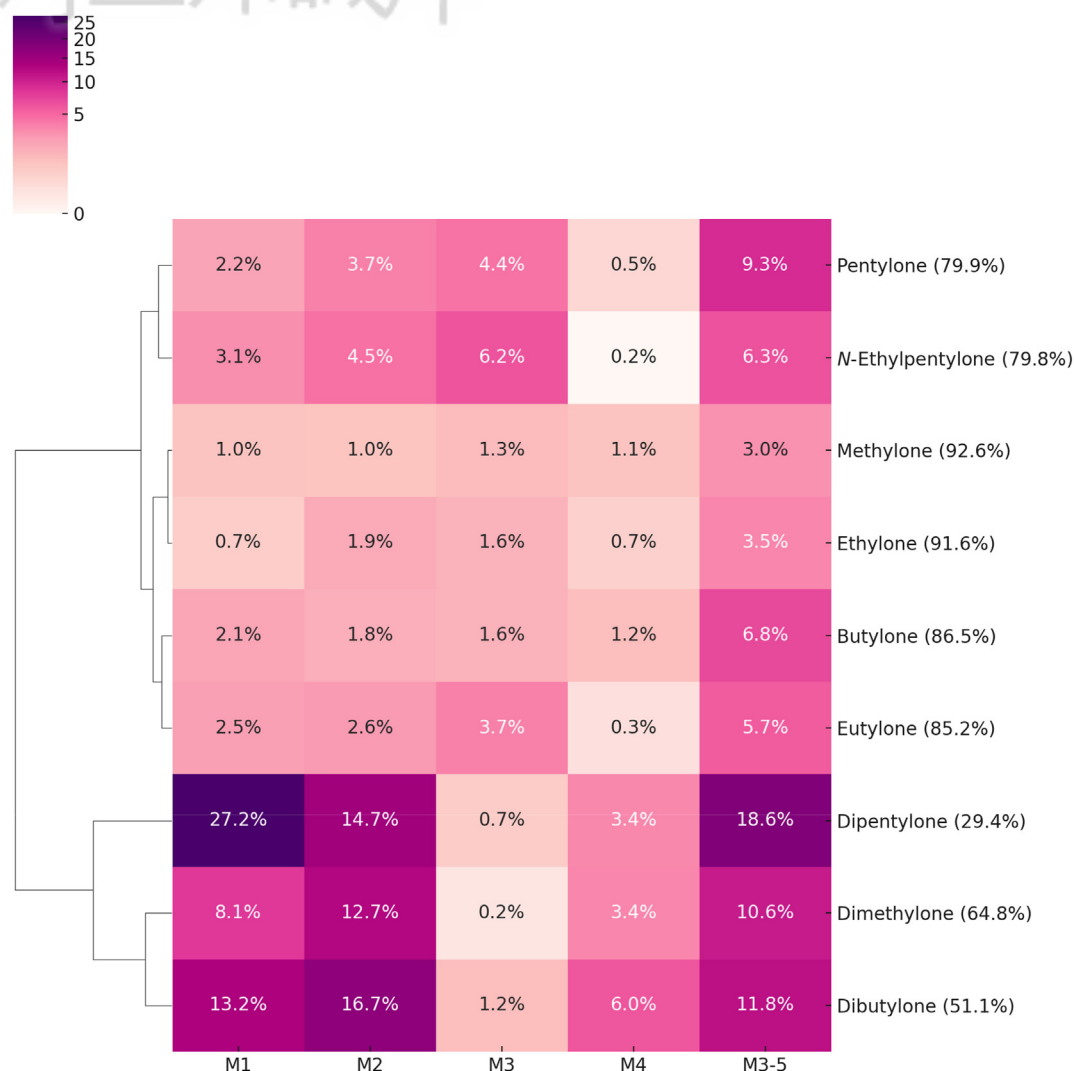


Fig. 2. Heatmap and hierarchical clustering dendrogram of the peak area ratios of the nine analytes and their metabolites (diastereomeric compounds were combined) in *in vitro* phase I metabolism.

similar metabolic trends, primarily metabolizing to M1, M2, and M3-5, and were clustered together accordingly. The notably low ratio of M3 was attributed to its subsequent metabolism to M3-5. Analytes [M], [E], [Eu], and [B] clustered together and were primarily metabolized to M3-5, followed by M3 or M2. [P] and [NEP] also showed metabolic similarities, reinforcing the role of M3-5 in their pathways. Beyond the clustering analysis, [DB] was observed to produce [B] metabolites ([B]M1, [B]M2, [B]M3, and [B]M3-5), while [DP] produced [P] metabolites ([P]M1, [P]M2, [P]M3, and [P]M3-5), indicating that the metabolic reactions proceeded sequentially. These findings expand the findings of earlier research, which primarily focused on single analytes or lacked detailed discussions of sequential metabolic pathways.

### 3.2. *In vitro* phase II metabolites

*In vitro* phase II metabolites are also summarized in Table 1. In addition to the phase I metabolites, M3 and M3-5 were further metabolized with glucuronic acid to form glucuronide conjugates, which were labeled as M3-g and M3-5-g, respectively. M3-5-g was found for all analytes, consistent with the findings of Kamata et al. [5], who highlighted the importance of glucuronidation as a significant phase II pathway. Because M3 was further metabolized to M3-5 and M3-5-g, M3 was not detected for any analyte except [DB], which contained trace amounts of the metabolite. Additionally, M3-g was observed for [NEP], [DM], [DB], and [DP]. The MS/MS spectra and fragment ions of M3-g and M3-5-g for [NEP], as shown in Fig. S1, confirm that after the



loss of glucuronide, the mass peaks of M3 and M3-5 become the secondary spectra of M3-g and M3-5-g, respectively.

The calculated peak area ratios of the nine analytes and their metabolites after phase II metabolism are summarized in the heatmap and hierarchical clustering dendrogram shown in Fig. S2. It is evident that Phase II metabolism reduced the peak area ratios of the parent compounds for all analytes. The calculated peak area ratios were 79.0% for [M], 76.5% for [B], 81.0% for [E], 76.6% for [P], 79.7% for [Eu], 76.0% for [NEP], 65.2% for [DM], 40.9% for [DB], and 35.2% for [DP]. This reduction in the peak area ratios relative to those observed following phase I metabolism reflects the increased formation of conjugated metabolites.

Similar to the results of phase I metabolism, analytes containing *N,N*-dimethylamino moieties (i.e., [DM], [DB], and [DP]) exhibited the lowest proportions of their parent compounds, in addition to higher metabolite ratios. M1 emerged as the predominant phase II metabolite, highlighting the role of *N*-dealkylation as a key pathway for these analytes. The main metabolites were M1, M2, and M3-5-g, with lower levels of M3-5 being detected owing to its further metabolism to M3-5-g. For the other analytes, the primary phase II metabolites were M3-5, M3-5-g, and M2, indicating a consistent metabolic trend. [DP] also produced [P] phase II metabolites ([P]M3-5-g). Overall, these findings demonstrate a consistent pattern of sequential metabolic reactions during phase II metabolism.

### 3.3. Distinguishing structural isomers and their metabolites

Structural isomer differentiation is critical for the accurate identification of synthetic cathinones and their metabolites, particularly in forensic toxicology. The nine analytes investigated in this study were grouped into three sets of structural isomers: Group 1 consisted of [DM], [E], and [B]; Group 2 comprised [DB], [P], and [Eu]; and Group 3 contained [DP] and [NEP]. In Group 1, [E]M1 is not an isomer of [DM] M1 or [B]M1; in Group 2, [Eu]M1 is not an isomer of [DB]M1 or [P]M1; and in Group 3, [NEP]M1 is not an isomer of [DP]M1. All the remaining metabolites were isomers. These isomers can be effectively distinguished by evaluating their RTs and mass spectral fragmentation patterns.

The accurate differentiation of these isomers relies on high-resolution MS, which provides precise mass measurements and supports inferences of fragmentation pathways. The proposed structures of each product ion and the corresponding fragmentation

pathways were consistent with those reported for other methylenedioxy compounds [25]. In the MS/MS spectra of the parent compounds, characteristic losses include the methylenedioxy group ( $\text{CH}_4\text{O}_2$ ), forming a phenyloxazole cation; water ( $\text{H}_2\text{O}$ ); neutral amine ( $\text{C}_2\text{H}_7\text{N}$ ), generating an alkenyldioxybenzoyloxonium cation; and  $\beta$ -keto cleavage, producing a methylenedioxybenzoyloxonium cation and an immonium ion. *N*-Dealkylation metabolites (M1) exhibit fragmentation patterns similar to those of their parent compounds, including the loss of a methylenedioxy group, water, and  $\beta$ -keto cleavage. In the case of the  $\beta$ -keto-reduced metabolites (M2), fragment ions were observed after the loss of water, the further loss of an alkyl group, and  $\alpha$ -cleavage between positions one and two, forming an immonium ion with additional water loss. Demethylenated metabolites (M3) show  $\beta$ -keto cleavage and the loss of one or two hydroxyl groups. Hydroxylated aliphatic metabolites (M4) exhibit  $\beta$ -keto cleavage, followed by CO loss. Demethylenated and *O*-methylated metabolites (M3-5) consistently show  $\beta$ -keto cleavage, hydroxyl group loss, and fragment ions formed by the loss of OH and  $\text{CH}_3\text{O}$ .

Figs. 3–5 show the respective full MS/MS spectra of Groups 1, 2, and 3 at a CE of 20 eV, along with the proposed structure of each fragment ion. In Group 1, the RT differences exceeded 0.25 min, allowing for approximate distinction between compounds. [E] and [B] displayed similar mass spectra; however, their metabolites, [E]M2 and [B]M2, were significantly different, enabling effective differentiation. The metabolites of [DM], [DM]M3 and [DM]M3-5, were clearly distinguishable from those of [E] and [B]. In Group 2, the RT differences exceeded 0.18 min. Although [P] and [Eu] shared similar mass spectra, their metabolites, [P]M2 and [Eu]M2, exhibited considerable differences. Furthermore, the metabolites of [DB], [DB]M3 and [DB]M3-5, were easily distinguishable from those of [P] and [Eu]. In Group 3, although the RT differences were minimal (0.07 min), significant variations in the MS/MS spectra allowed for clear differentiation between the compounds. Differences in the MS/MS spectra and RTs of the isomers and their metabolites highlight the requirement for a database that integrates both accurate drug detection and isomer identification in forensic applications.

### 3.4. Analysis of urine samples in relation to the *in vitro* metabolism results

A total of 29 urine samples were analyzed, including 12 samples containing [M], 8 containing [DB], 8 containing [NEP], and 1 containing [DP], to

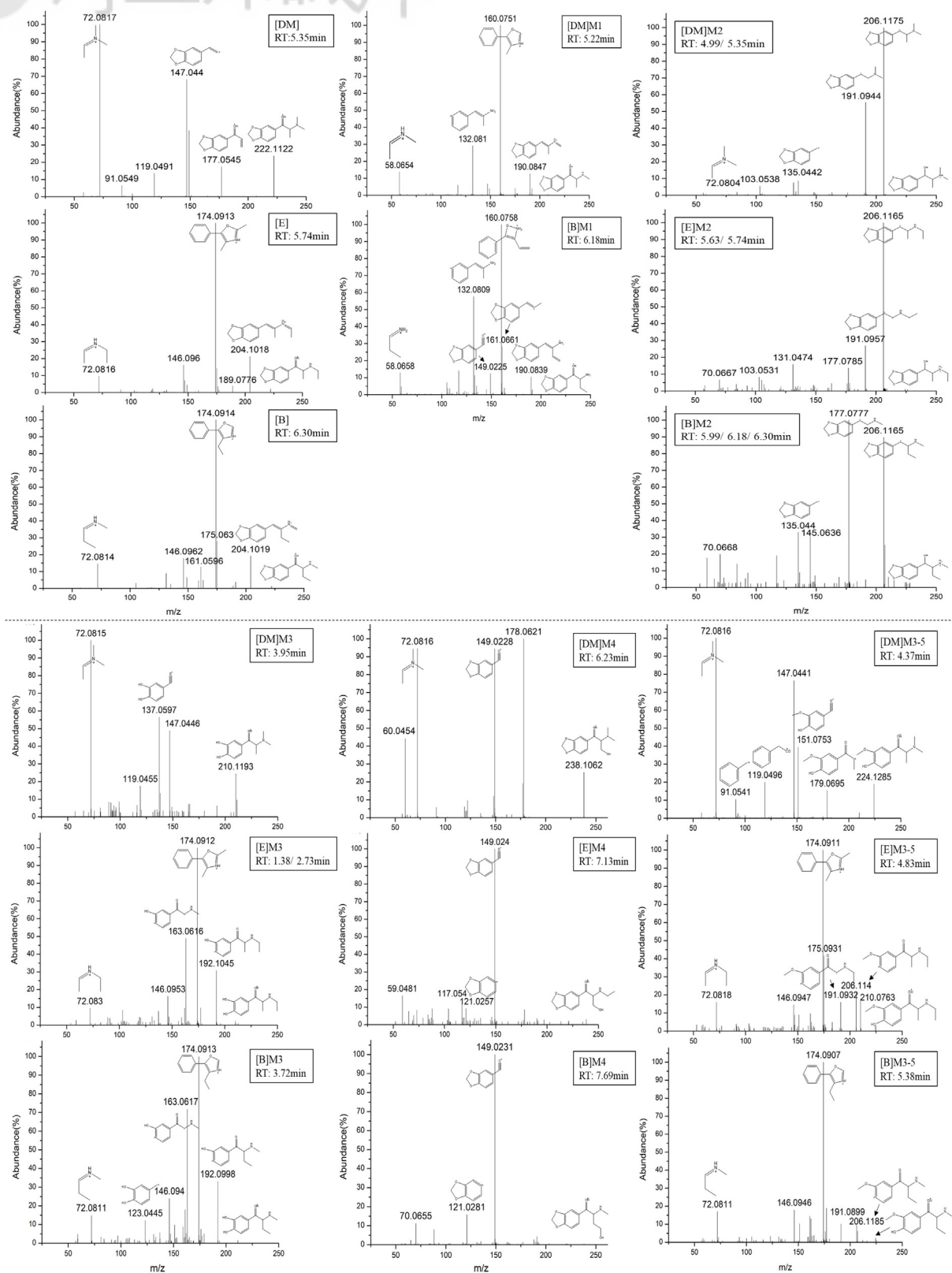


Fig. 3. Full MS/MS spectra (collision energy: 20 eV) of dimethylone (DM), ethylone (E), butylone (B), and their metabolites. The possible structures of the corresponding fragment ions are also shown.

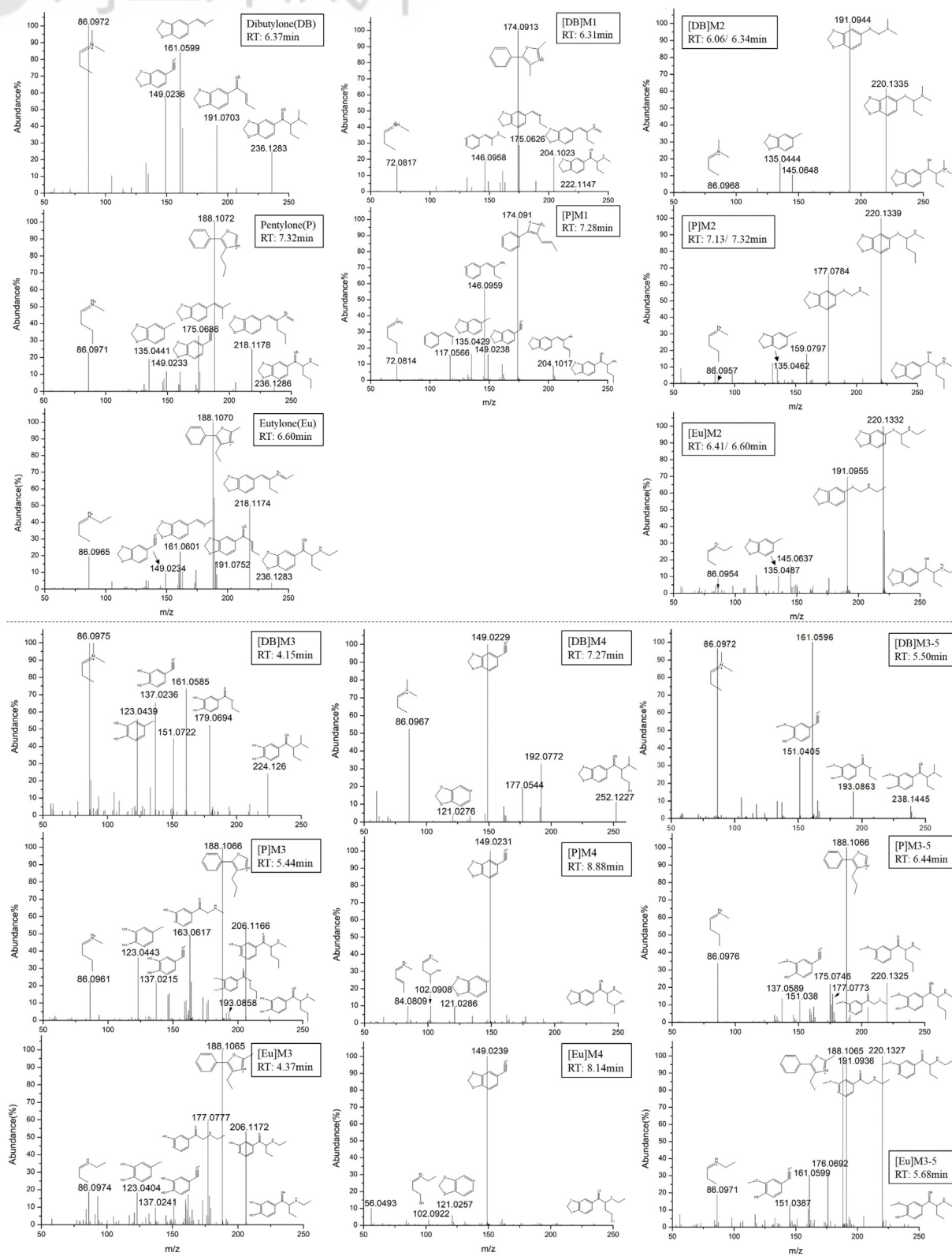


Fig. 4. Full MS/MS spectra (collision energy: 20 eV) of dibutylone ([DB]), eutylone ([Eu]), pentylone ([P]), and their metabolites. The possible structures of the corresponding fragment ions are also shown.

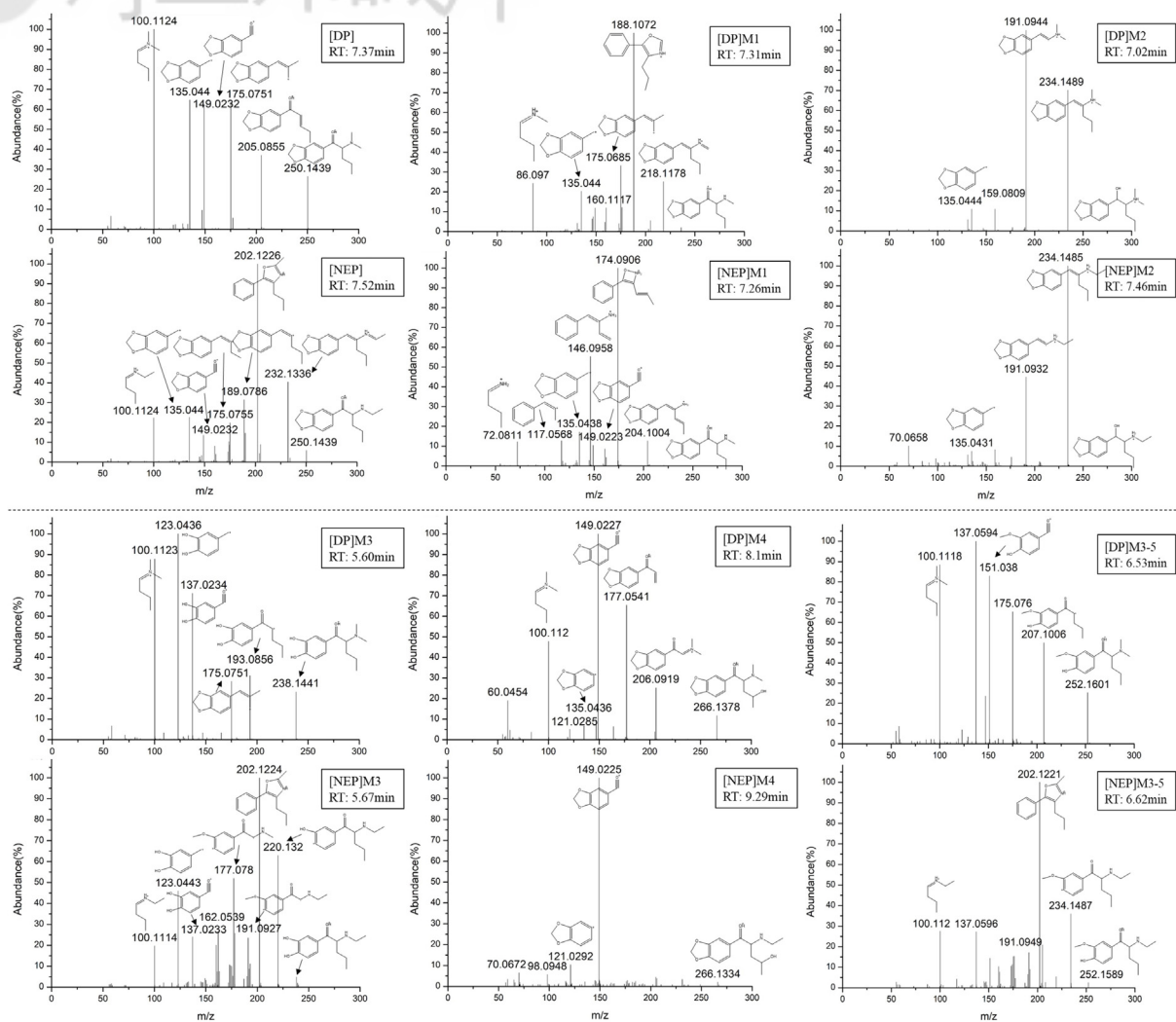


Fig. 5. Full MS/MS spectra (collision energy: 20 eV) of dipentylone ([DP]), N-ethylpentylone ([NEP]), and their metabolites. The possible structures of the corresponding fragment ions are also shown.

investigate the detection of their respective metabolites. Urine sample analysis confirmed the *in vitro* metabolism results, demonstrating consistency across the RTs (within  $\pm 2.5\%$ ), accurate precursor ion masses, and secondary mass spectra for all analyzed metabolites. Figs. 6–8 corresponding to each compound depicts the peak area ratios of the parent drug and its metabolites, with the samples arranged from highest to lowest parent drug peak area ratios.

#### 3.4.1. Methylone

Fig. 6 shows the peak area ratios of [M] and its metabolites across 12 urine samples (M-1–M-12). The [M] concentration varied widely over the range of 7–10,154 ng/mL (mean = 1689 ng/mL; median = 525 ng/mL). Among the detected metabolites, [M]M1 exhibited the lowest ratio in all

samples, while [M]M2 was the main metabolite, and its concentration increased as the ratio of [M] decreased. [M]M3-5 also increased as the ratio of [M] decreased, but generally had a lower concentration than [M]M2. [M]M4 was only present in sample M-7, which had the highest concentration of [M]. These observations suggest some variability in the metabolic profiles of individuals, which may be influenced by differences in the dosage, frequency of use, or metabolic capacity. Unlike the findings of Pedersen et al. [9] and Kamata et al. [5,6], which did not emphasize [M]M2, our study revealed [M]M2 both *in vitro* and in urine samples, indicating that  $\beta$ -ketone reduction is a key pathway for [M] metabolism.

Notably, the ratio and concentration of [M] were inconsistent across the samples, possibly because the individuals suspected of drug use in Taiwan



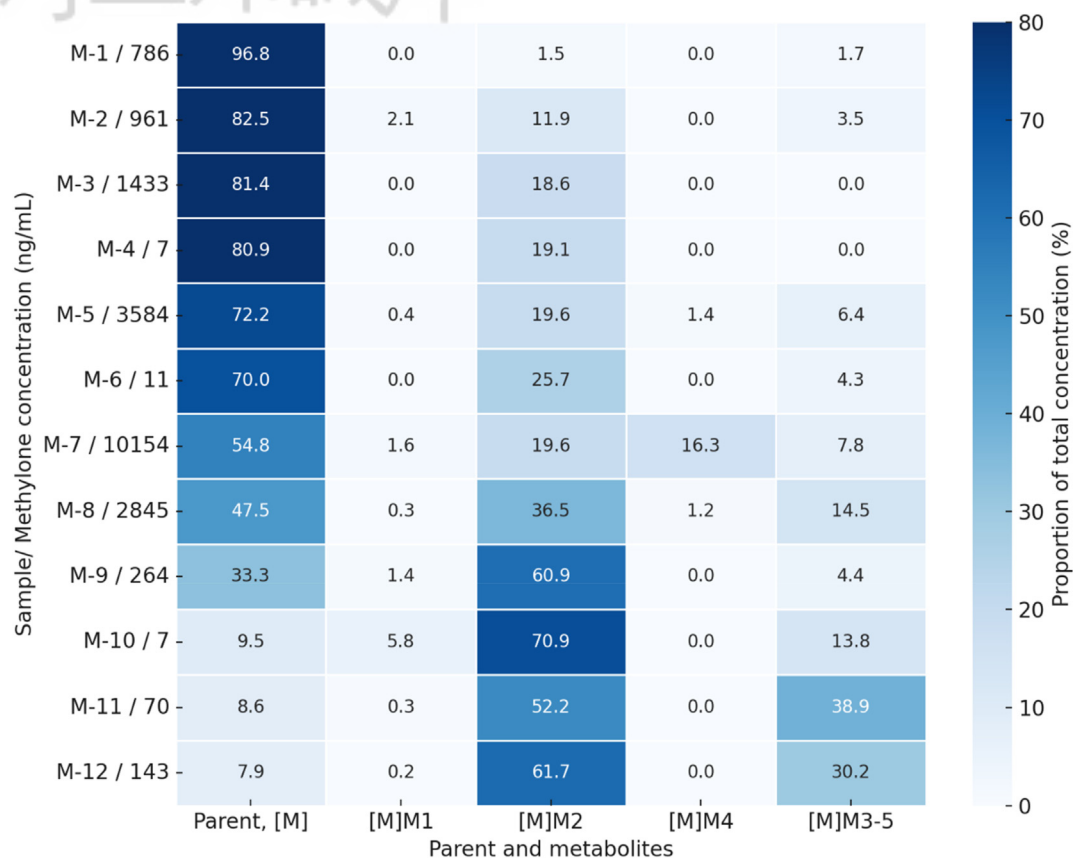


Fig. 6. Peak area ratios of methylone ([M]) and its metabolites across 12 urine samples (M-1–M-12).

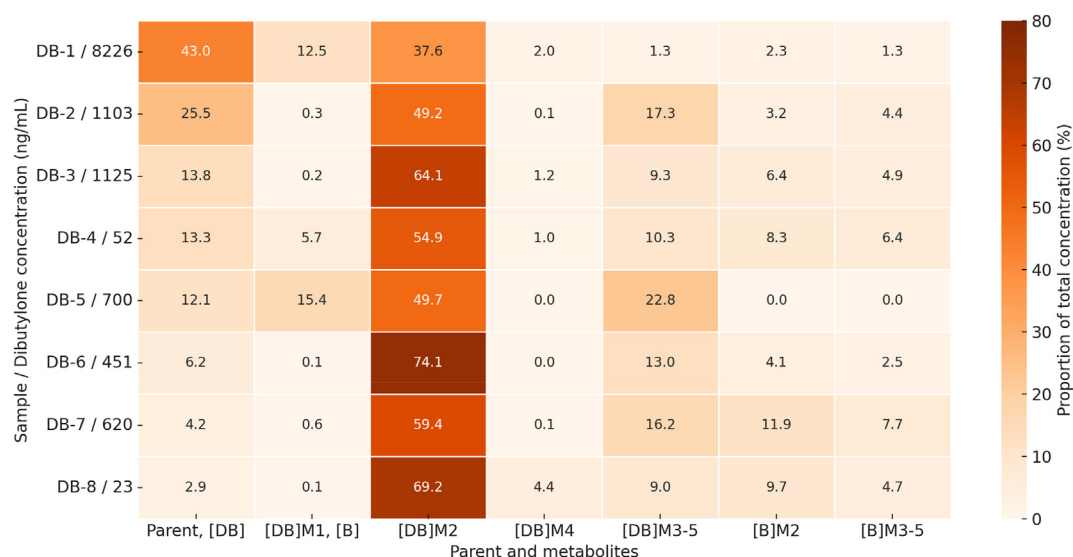


Fig. 7. Peak area ratios of dibutylone ([DB]) and its metabolites across eight urine samples (DB-1–DB-8).

consumed different concentrations of synthetic cathinones in their coffee packets. This inconsistency suggests that absolute [M] concentrations are not a reliable indicator of metabolic profile. Instead, the peak area ratios of [M] and its metabolites

provide a more robust approach for understanding individual metabolic profiles. For example, a higher ratio of [M]M2 relative to [M] may indicate a more extensive metabolic activity. Moreover, key metabolites such as [M]M2 and [M]M3-5 can provide

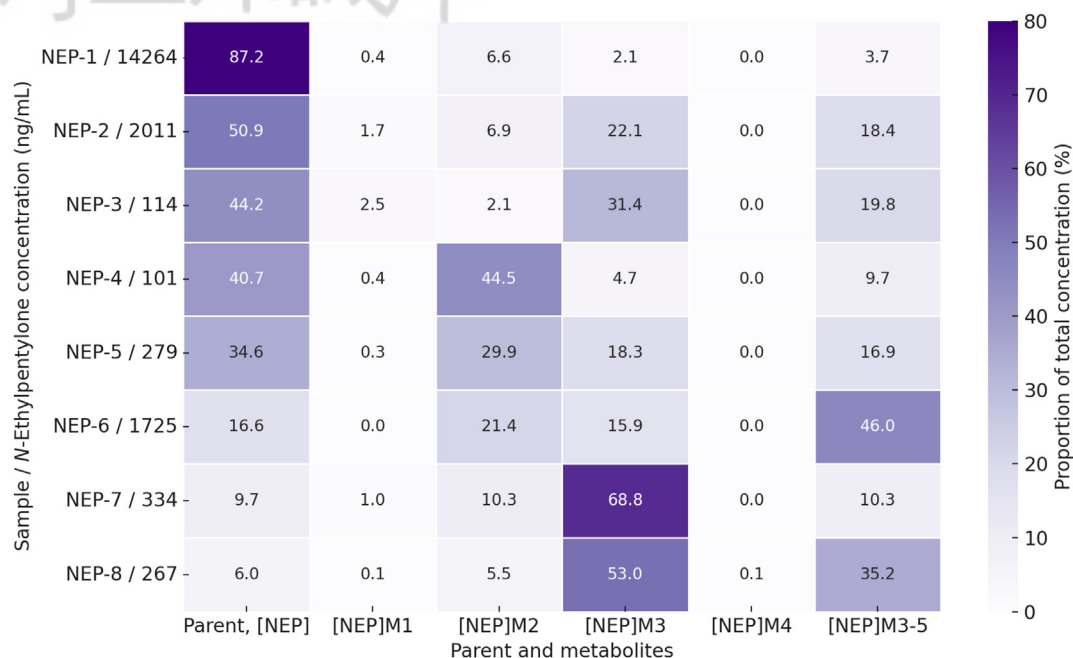


Fig. 8. Peak area ratios of N-ethylpentylone ([NEP]) and its metabolites across eight urine samples (NEP-1–NEP-8).

valuable information for identifying [M] use, even when the parent drug concentration is low or variable.

#### 3.4.2. Dibutylone

Fig. 7 shows the peak area ratios of [DB] and its metabolites across eight urine samples (DB-1–DB-8). The [DB] concentrations in the eight samples ranged from 23 to 8226 ng/mL (mean = 1537 ng/mL; median = 600 ng/mL). Because [DB] can be metabolized to [B] and both substances may be consumed simultaneously, the metabolic profile for [DB] is more complex. This complexity underscores the importance of analyzing both parent compounds and metabolites to effectively identify drug use. Among the detected metabolites, [DB]M1 had a ratio of less than 15.4% and was present in very low levels in five samples. [DB]M2 was the main metabolite in all samples, and had a much higher ratio than [DB] except DB-1. The finding that the ratio of [DB]M2 was consistently higher than that of [DB] suggests that  $\beta$ -ketone reduction is a key metabolic pathway, consistent with the findings of Krotulski et al. [12]. These results therefore indicate that [DB]M2 is a reliable indicator of [DB] metabolism, particularly when the parent drug concentration is low. Except in sample DB-1, [DB]M3-5 was the second most common metabolite in all samples. The variation in the metabolite profiles of [DB] across the samples may reflect individual metabolic differences, differences in dosage, or the mixed use of [DB] and [B]. For instance, DB-1 exhibited a high

parent drug ratio, suggesting a limited metabolism, whereas the other samples showed lower [DB] ratios with a shift toward higher proportions of other metabolites, particularly [DB]M2 and [DB]M3-5. [DB]M4 had a ratio of less than 4.5% and was present in low levels in all samples. Although the concentration of [B] was very low, most of its metabolites could still be detected. More specifically, [B]M2 and [B]M3-5 were detected in all samples except DB-5. Notably, [B]M2 was generally more abundant than [B]M3-5, indicating a similar metabolic trend for [DB] and [B]. No [B] metabolites were detected in DB-5, where [DB]M1 was identified as the predominant metabolite. This finding may reflect a lower extent of metabolism or differences in drug usage. However, the simultaneous use of [DB] and [B] must still be considered. Krotulski et al. [12] analyzed urine samples and found five metabolites: [DB]M1, [DB]M2, [DB]M3, the *N*-dealkylation and *N*-dealkylation metabolite, and the demethylenation and  $\beta$ -ketone reduction metabolite; among these, [DB]M2 was the primary metabolite, followed by [DB]M1. In the present study, a higher ratio of [DB]M3-5 was observed, which may be due to the inclusion of cytosol in the experimental setup.

#### 3.4.3. N-ethylpentylone

Fig. 8 shows the peak area ratios of [NEP] and its metabolites across eight urine samples (NEP-1–NEP-8). The [NEP] concentrations in the eight samples ranged from 101 to 14,246 ng/mL (mean = 2387 ng/mL; median = 307 ng/mL). Among

the detected metabolites, [NEP]M1 was consistently present in low levels in all samples. Because [NEP]M3 is further metabolized to [NEP]M3-5, their combined proportions were considered. [NEP]M3 and [NEP]M3-5 were the main metabolites in all samples except NEP-1 and NEP-4, in which [NEP]M2 was the main metabolite. The ratios of [NEP]M3 and [NEP]M3-5 increased substantially as the ratio of [NEP] decreased. This trend suggests that demethylenation followed by *O*-methylation plays a significant role in the metabolic transformation of [NEP], and provides reliable markers for [NEP] usage, even when the parent drug concentration is low. However, individual differences and varying patterns of drug use may contribute to the observed variability in these ratios. Krotulski et al. [13] similarly identified four metabolites ([NEP]M1, [NEP]M2, [NEP]M3, and [NEP]M4) in both blood and saliva samples, with [NEP]M2 being the predominant metabolite. Because blood and saliva predominantly contain early-stage metabolites, these findings are consistent with our finding that [NEP]M2 was the main metabolite, particularly for NEP-4 and NEP-5. Notably, our detection of [NEP]M3-5, which was absent in previous studies, may be attributed to the inclusion of cytosol in our *in vitro* experimental design, thereby enabling the identification of further metabolites.

#### 3.4.4. Dipentylone

A single urine sample containing [DP] was analyzed. The peak area ratio of [DP] was 7.2%, with the following metabolite ratios: 12.7% [DP]M1 (also [P]), 26.5% [DP]M2, 16.8% [DP]M3, 16.1% [DP]M4, 1.4% [DP]M3-5, 2.4% [P]M2, and 16.8% [P]M3-5. Similar to [DB], [DP] can be metabolized to [P]. Although the [DP] concentration was low, the presence of multiple [DP]-derived metabolites provides conclusive evidence of its administration. Fogarty et al. [15] also detected [P] in 18 postmortem cases involving [DP]. These findings emphasize the necessity of including [DP]-specific metabolites such as [DP]M2 and [DP]M3 as markers for accurate differentiation. The detection of these metabolites in the present study validates their utility in forensic analyses.

## 4. Discussion

The effective differentiation of structural isomers and their metabolites was achieved using high-resolution MS by leveraging differences in the RTs and fragmentation patterns. For example, differences in the RTs among isomers such as [DM], [E], and [B] (Group 1) exceeded 0.2 min, allowing approximate

distinction between parent drugs. Furthermore, significant variations in the fragmentation patterns of metabolites such as [E]M2 and [B]M2 in Group 1 and [DB]M3 and [P]M3 in Group 2 provided robust markers for distinguishing the isomers. In Group 3, differentiation was achieved primarily through significant variations in the MS/MS spectra. Building on the differentiation of structural isomers, the analysis of urine samples revealed further insights into the metabolism of methylenedioxy-substituted synthetic cathinones, demonstrating a strong consistency between the *in vitro* and *in vivo* findings. [M], as the parent compound, and its main metabolite, [M]M2, were the predominant compounds in the collected samples. As the ratio of [M] decreased, the ratios of [M]M2 and [M]M3-5 increased, reflecting sequential metabolic pathways. For [DB], the *in vitro* findings demonstrated that *N*-dealkylation and subsequent metabolism to [B] metabolites, such as [B]M2 and [B]M3-5, were common pathways. This trend was consistent with the results of urine sample analysis, in which [DB]M1 was detected predominantly in samples with high parent drug concentrations, such as DB-1, whereas [DB]M2 and [DB]M3-5 were dominant in other samples. The presence of [B] metabolites highlights the complexity of [DB] metabolism and the need to distinguish between co-administered substances and their sequential metabolic transformations. [NEP] metabolism exhibited a similar trend, with [NEP]M2 dominating in samples with higher parent drug concentrations and [NEP]M3 and [NEP]M3-5 increasing as the parent drug levels declined. In some cases, the levels of [NEP]M3 exceeded those of [NEP]M3-5, suggesting a slower *O*-methylation process, which differs slightly from the *in vitro* results. For [DP], the single analyzed urine sample demonstrated the presence of both [DP] and [P] metabolites, confirming the sequential metabolic conversion of [DP] into [P]. The predominant metabolites, [DP]M2, [DP]M3, and [P]M3-5, highlight the overlap in the metabolic pathways for these two substances. The relatively low proportion of [DP]M3-5 compared with those of the other metabolites suggests either slower conversion from [DP]M3 or its further metabolism to [P]M3-5.

As mentioned earlier, in Taiwan, synthetic cathinones are often mixed with coffee powder and abused in the form of “coffee packets” [4]. This type of administration could result in a wide variations in drug concentrations, as observed in the urine samples: 7–10,154 ng/mL for [M], 23–8226 ng/mL for [DB], and 101–14,264 ng/mL for [NEP]. Despite this variation, however, this study highlights the critical role of metabolites, particularly M2

( $\beta$ -ketone reduction) and M3-5 (demethylenation followed by *O*-methylation), in extending the detection window for synthetic cathinones. The metabolic trends for M3-5 align with the findings of Zaitzu et al. [8], while the minor pathway involving M2 supports the observations of Krotulski et al. [12–14]. In cases where the parent drug concentration is below Taiwan's legal threshold of 50 ng/mL, the detection of multiple metabolites could provide compelling evidence to confirm drug use. For instance, samples with low parent drug concentrations, such as [M] in M-4 (7 ng/mL), M-6 (11 ng/mL), M-10 (7 ng/mL), and [DB] in DB-8 (23 ng/mL), were successfully identified through the detection of multiple metabolites, including [M] M2 and [M]M3-5 for [M], and [DB]M2, [DB]M3-5, and [B]M2 for [DB]. The identification of multiple metabolites not only reinforces the reliability of the findings but also extends the detection window, underscoring the importance of metabolite analysis in cases with low parent drug concentrations.

Despite the strong consistency between the *in vitro* and *in vivo* results, the inability to detect phase II metabolites, such as M3-5-g, in urine samples owing to extraction limitations emphasizes an area for further improvement. Additionally, the variability in metabolite ratios and parent compound

concentrations observed across the urine samples may reflect differences in consumption patterns and time intervals, unlike under controlled *in vitro* conditions. Given that current NPS detection methods for urine focus primarily on the parent compound, this study recommends incorporating metabolite screening to improve detection accuracy and reduce the risk of isomer misidentification. This approach would enable a retrospective analysis without the requirement for sample reanalysis, allowing forensic experts to review the original data of analytes and metabolites to confirm substance use. The proposed approach provides a reliable tool for both retrospective and prospective forensic analyses, offering a practical solution to the complex analytical challenges associated with the detection of synthetic cathinones.

### Funding statement

This study was supported by the Ministry of the Interior of Taiwan (ROC) [grant numbers 110-0805-10-17-01, 2021; 111-0805-02-28-01, 2022; and 112-0805-02-28-01, 2023].

### Supplementary material.

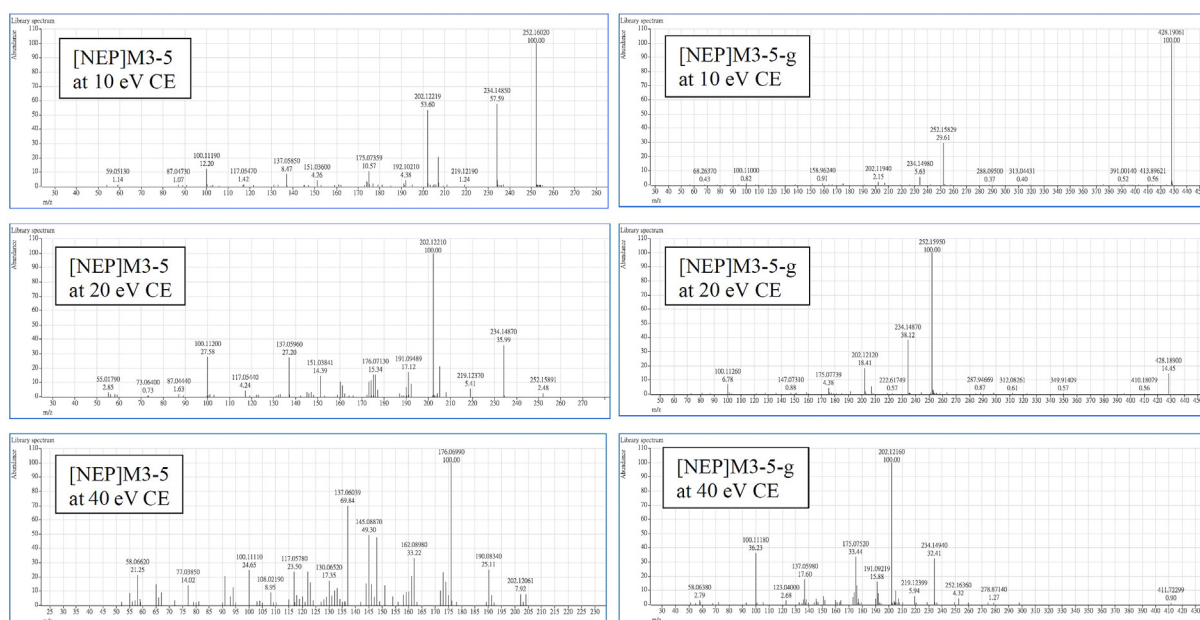


Fig. S1. Full MS/MS spectra of [NEP]M3-5 and [NEP]M3-5-g at 10, 20, and 40 eV CE.



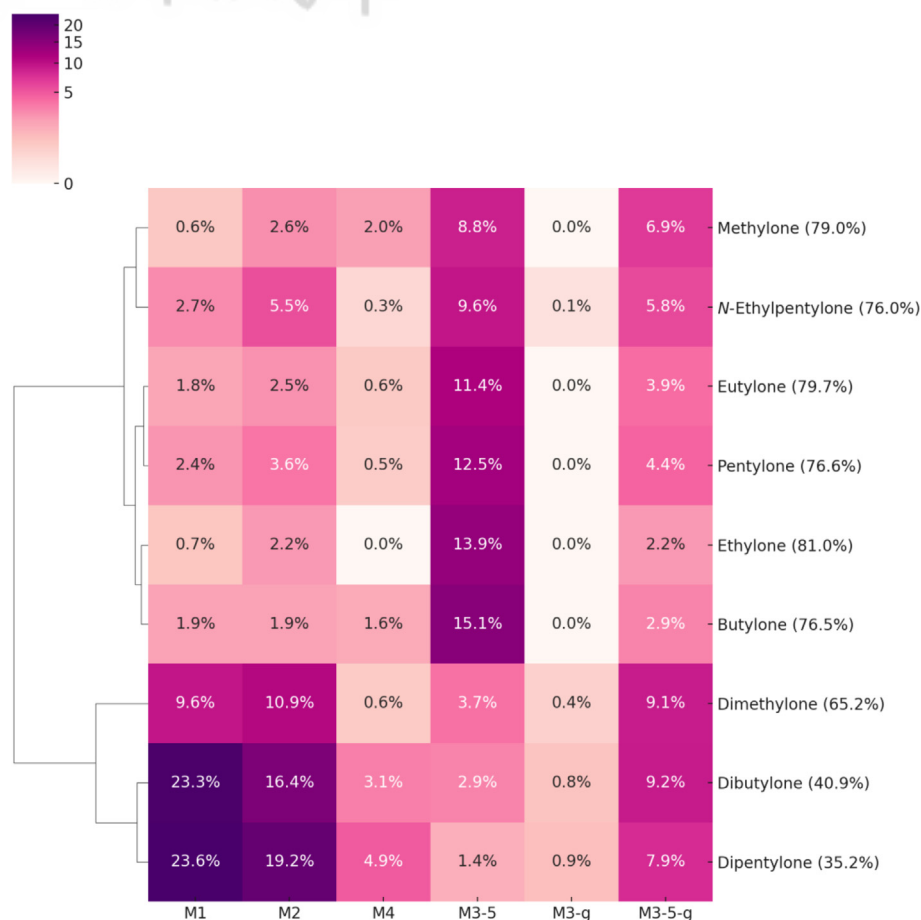


Fig. S2. Heatmap and hierarchical clustering dendrogram of the peak area ratios of the nine analytes and their metabolites (diastereomeric compounds were combined) in *in vitro* phase II metabolism.

## References

- [1] United Nations Office on Drugs and Crime. World drug report. 2024. Available at: <https://www.unodc.org/unodc/en/data-and-analysis/world-drug-report-2024.html>. [Accessed 28 September 2024].
- [2] United Nations Office on Drugs and Crime. World drug report. 2022. Available at: <https://www.unodc.org/unodc/en/data-and-analysis/world-drug-report-2022.html>. [Accessed 28 September 2024].
- [3] Taiwan Ministry of Health and Welfare. List of New psychoactive substances (NPS) detected in Taiwan. Available at <https://www.fda.gov.tw/tc/site.aspx?sid=9958&r=897181954>. [Accessed September 28, 2024].
- [4] Feng LY, Li JH. New psychoactive substances in Taiwan: challenges and strategies. *Curr Opin Psychiatr* 2020;33: 306–11.
- [5] Kamata HT, Shima N, Zaitzu K, Kamata T, Miki A, Nishikawa M, et al. Metabolism of the recently encountered designer drug, methylone, in humans and rats. *Xenobiotica* 2006;36:709–23.
- [6] Kamata HT, Shima N, Zaitzu K, Kamata T, Nishikawa M, Katagi M, et al. Simultaneous analysis of new designer drug, methylone, and its metabolites in urine by gas chromatography-mass spectrometry and liquid chromatography-electrospray ionization mass spectrometry. *Jpn J Forensic Sci* 2007;12:97–106.
- [7] Uralets V, Rana S, Morgan S, Ross W. Testing for designer stimulants: metabolic profiles of 16 synthetic cathinones excreted free in human urine. *J Anal Toxicol* 2014; 38:233–41.
- [8] Zaitzu K, Katagi M, Kamata HT, Kamata T, Shima N, Miki A, et al. Determination of the metabolites of the new designer drugs bk-MBDB and bk-MDEA in human urine. *Forensic Sci Int* 2009;188:131–9.
- [9] Pedersen AJ, Petersen TH, Linnet K. In vitro metabolism and pharmacokinetic studies on methylone. *Drug Metab Dispos* 2013;41:1247–55. <https://doi.org/10.1124/dmd.112.050880>.
- [10] Meyer MR, Wilhelm J, Peters FT, Maurer HH. Beta-keto amphetamines: studies on the metabolism of the designer drug mephedrone and toxicological detection of mephedrone, butylone, and methylone in urine using gas chromatography-mass spectrometry. *Anal Bioanal Chem* 2010; 397:1225–33.
- [11] Mueller DM, Rentsch KM. Generation of metabolites by an automated online metabolism method using human liver microsomes with subsequent identification by LC-MS(n), and metabolism of 11 cathinones. *Anal Bioanal Chem* 2012; 402:2141–51.
- [12] Krotulski AJ, Mohr ALA, Papsun DM, Logan BK. Dibutylone (bk-DMBDB): intoxications, quantitative confirmations and metabolism in authentic biological specimens. *J Anal Toxicol* 2018;42:437–45.
- [13] Krotulski AJ, Papsun DM, De Martinis BS, Mohr ALA, Logan BK. 2N-Ethyl pentylone (ephylone) intoxications: quantitative confirmation and metabolite identification in authentic human biological specimens. *J Anal Toxicol* 2018; 42:467–75.

- [14] Krotulski AJ, Papsun DM, Chronister CW, Homan J, Crosby MM, Hoyer J, et al. Eutylone intoxications—An emerging synthetic stimulant in forensic investigations. *J Anal Toxicol* 2021;45:8–20.
- [15] Fogarty MF, Krotulski AJ, Papsun DM, Walton SE, Lamb M, Truver MT, et al. 2N,N-Dimethylpentylone (dipentylone)—a new synthetic cathinone identified in a postmortem forensic toxicology case series. *J Anal Toxicol* 2023;47:753–61.
- [16] Yeh YL, Wang SM. Quantitative determination and metabolic profiling of synthetic cathinone eutylone in vitro and in urine samples by liquid chromatography tandem quadrupole time-of-flight mass spectrometry. *Drug Test Anal* 2022;14:1325–37.
- [17] Peters FT, Meyer MR. In vitro approaches to studying the metabolism of new psychoactive compounds. *Drug Test Anal* 2011;3:483–95.
- [18] Jia L, Liu X. The conduct of drug metabolism studies considered good practice (II): in vitro experiments. *Curr Drug Metab* 2007;8:822–9.
- [19] Walsky RL, Bauman JN, Bourcier K, Giddens G, Lapham K, Negahban A, et al. Optimized assays for human UDP-glucuronosyltransferase (UGT) activities: altered alamethicin concentration and utility to screen for UGT inhibitors. *Drug Metab Dispos* 2012;40:1051–65.
- [20] Presley BC, Logan BK, Jansen-Varnum SA. Phase I metabolism of synthetic cannabinoid receptor agonist PX-1 (5F-APP-PICA) via incubation with human liver microsomes and UHPLC–HRMS. *Biomed Chromatogr* 2020;34:e4786.
- [21] Presley BC, Logan BK, Jansen-Varnum SA. In vitro metabolic profile elucidation of synthetic cannabinoid APP-CHMI-NACA (PX-3). *J Anal Toxicol* 2020;44:226–36.
- [22] Paul M, Bleicher S, Guber S, Ippisch J, Poletini A, Schultis W. Identification of phase I and II metabolites of the new designer drug  $\alpha$ -pyrrolidinohexiophenone ( $\alpha$ -PHP) in human urine by liquid chromatography quadrupole time-of-flight mass spectrometry (LC-QTOF-MS). *J Mass Spectrom* 2015;50:1305–17.
- [23] Zaitse K, Katagi M, Tsuchihashi H, Ishii A. Recently abused synthetic cathinones,  $\alpha$ -pyrrolidinophenone derivatives: a review of their pharmacology, acute toxicity, and metabolism. *Forensic Toxicol* 2014;32:1–8.
- [24] Eh-Haj BM. Metabolic N-dealkylation and N-oxidation as elucidators of the role of alkylamino moieties in drugs acting at various receptors. *Molecules* 2021;26:1917.
- [25] Fornal E. Identification of substituted cathinones: 3, 4-Methylenedioxy derivatives by high performance liquid chromatography–quadrupole time of flight mass spectrometry. *J Pharm Biomed Anal* 2013;81:13–9.